EBioMedicine 18 (2017) 188–198

Contents lists available at ScienceDirect

EBioMedicine

journal homepage: www.ebiomedicine.com

Research Paper

Batf3-dependent CD8α$^+$ Dendritic Cells Aggravates Atherosclerosis via Th1 Cell Induction and Enhanced CCL5 Expression in Plaque Macrophages

Yalin Li [a], Xueyan Liu [a], Wei Duan [a], Hua Tian [b], Guangming Zhu [a], Hao He [a], Shutong Yao [b], Shuying Yi [a], Wengang Song [a,*], Hua Tang [a,*,1]

[a] Institute of Immunology, Taishan Medical University, Taian, Shandong, China
[b] Key Laboratory of Atherosclerosis in Universities of Shandong and Institute of Atherosclerosis, Taishan Medical University, Shandong, China

ARTICLE INFO

Article history:
Received 1 October 2016
Received in revised form 24 March 2017
Accepted 4 April 2017
Available online 6 April 2017

Keywords:
Batf3
CD8α$^+$ DCs
Th1 cells
CCL5
Atherosclerosis

ABSTRACT

Dendritic cells (DCs) play an important role in controlling T cell-mediated adaptive immunity in atherogenesis. However, the role of the basic leucine zipper transcription factor, ATF-like 3 (Batf3)-dependent CD8α$^+$ DC subset in atherogenesis remains unclear. Here we show that *Batf3*$^{-/-}$*Apoe*$^{-/-}$ mice, lacking CD8α$^+$ DCs, exhibited a significant reduction in atherogenesis and T help 1 (Th1) cells compared with *Apoe*$^{-/-}$ controls. Then, we found that CD8α$^+$ DCs preferentially induce Th1 cells via secreting interleukin-12 (IL-12), and that the expression of interferon-gamma (IFN-γ)or chemokine (C-C motif) ligand 5 (CCL5) in aorta were significantly decreased in *Batf3*$^{-/-}$*Apoe*$^{-/-}$ mice. We further demonstrated that macrophages were the major CCL5-expressing cells in the plaque, which was significantly reduced in *Batf3*$^{-/-}$*Apoe*$^{-/-}$ mice. Furthermore, we found CCL5 expression in macrophages was promoted by IFN-γ. Finally, we showed that *Batf3*$^{-/-}$*Apoe*$^{-/-}$ mice displayed decreased infiltration of leukocytes in the plaque. Thus, CD8α$^+$ DCs aggravated atherosclerosis, likely by inducing Th1 cell response, which promoted CCL5 expression in macrophages and increased infiltration of leukocytes and lesion inflammation.

1. Introduction

Atherosclerosis is a chronic, systemic inflammatory disease characterized by immune cells accumulation in the arterial wall and formation of atherosclerotic plaques (Chaudhari et al., 2015). Among these cells, macrophages have been well-characterized for their ability to phagocytose oxidized low density lipoprotein (OxLDL) and become foamy cells (Moore and Tabas, 2011). It has also been suggested that macrophages can secrete inflammatory cytokines and chemokines that are likely related to the promotion of lipoprotein retention and the accumulation of immune cells in the arterial wall (Moore and Tabas, 2011). One in vitro study demonstrated that in response to OxLDL stimuli, macrophages up-regulated mRNA encoding CXC chemokine ligand (CXCL) 1, CXCL2, and chemokine (C-C motif) ligand 5 (CCL5 or Rantes) (Stewart et al., 2010). The majority of these chemokines promote atherogenesis via the accumulation of inflammatory cells (Rolin and Maghazachi, 2014). In particular, treatment with a CCL5 antagonist was found to inhibit the recruitment of T cells and macrophages into the plaque area, and alleviate atherosclerosis (Veillard et al., 2004). However, which cells or molecules promote macrophages secreting CCL5 to enhance leukocyte infiltrating into atherosclerotic plaque in vivo, remains unknown.

A T cell-mediated adaptive immune response also plays an important role in atherosclerosis, as pro and anti-atherogenic CD4$^+$T cell subsets, as well as their signature cytokines have been defined (Lahoute et al., 2011; Smith et al., 2010; Subramanian et al., 2013). In particular, evidence shows that CD4$^+$T helper 1 (Th1) cells and their key cytokine, interferon gamma (IFN-γ) are pro-atherosclerotic (Benagiano et al., 2003; Buono et al., 2005). Apolipoprotein-E deficient mice (*Apoe*$^{-/-}$) that lack T-bet (a Th1 cell-differentiating transcription factor) or the IFN-γ receptor have demonstrated a reduction in atherosclerosis development (Buono et al., 2005; Gupta et al., 1997). Moreover, mice that receive exogenous IFN-γ have a larger atherosclerotic lesion area than the control mice (Whitman et al., 2000). However, during atherosclerotic progress, it is unclear how the Th1 cell response is generated, and whether IFN-γ regulates macrophage activation involved in atherosclerotic plaque formation.

DCs have long been recognized as the most potent antigen-presenting cells and are composed of distinct subsets, of which development is specifically regulated by distinct transcriptional factors. For example, interferon regulatory factor 4 (IRF4) and Notch2 are critical for CD11b$^+$ DCs generation, whereas IRF8 and Batf3 are essential for CD8a$^+$ DCs development (Mildner and Jung, 2014). It has been suggested that DCs

* Corresponding authors.
E-mail addresses: wgsong@tsmc.edu.cn (W. Song), htang@tsmc.edu.cn (H. Tang).
[1] Lead Contact.

http://dx.doi.org/10.1016/j.ebiom.2017.04.008

play an important role in controlling the T cell-mediated adaptive immune response to regulate atherogenesis (Choi et al., 2011; Gautier et al., 2009; Koltsova et al., 2012; Subramanian et al., 2013; Weber et al., 2011). Moreover, different DC subsets have distinct function in modulating different types of adaptive immunity (Choi et al., 2011; Sage et al., 2014; Weber et al., 2011). For instance, a CCL17-expressing $CD11b^+$ DCs subset promotes atherosclerosis through the inhibition of regulatory T cell (Treg) expansion in lymphoid tissues (Weber et al., 2011). In addition, in mouse models of genetic and high-fat/cholesterol diet-induced dyslipidemia, $CD8\alpha^-$ DCs preferentially induced a Th2 response (Shamshiev et al., 2007). Although the role of $CD8\alpha^+$ DCs in atherosclerosis has been suggested, one study suggested the protective role of $CD8\alpha^+$ DCs but another showed no functions of $CD8\alpha^+$ DCs in atherosclerosis (Choi et al., 2011; Legein et al., 2015). These contradicting results on their role in controlling T cell-mediated atherosclerosis were assiocated with experimental mice that had different gene difficiency. Thus, the function of $CD8a^+$ DCs in atherosclerosis remains to be elucidated.

In the current study, to clarify the role of $CD8a^+$ DCs in atherosclerosis, a double knockout $Batf3^{-/-}Apoe^{-/-}$ mouse was generated and fed with a Western diet. Our findings indicate an important role of Batf3-dependent $CD8\alpha^+$ DCs in controlling Th1 cell cytokine production, and IFN-γ-dependent chemokine CCL5 expression by macrophages during atherosclerotic progression.

2. Materials and Methods

2.1. Mice

$Apoe^{-/-}$ mice(RRID:IMSR_JAX:002052), OT-II mice(RRID:IMSR_JAX:004194)on a C57BL/6 background, and *Batf3* deficient mice $Batf3^{-/-}$ (RRID:IMSR_JAX:013755)were obtained from the Jackson Laboratory (Bar Harbor, ME). $Batf3^{-/-}$ mice were crossed with $Apoe^{-/-}$ mice to generate double knockout mice $Batf3^{-/-}Apoe^{-/-}$. $Batf3^{-/-}Apoe^{-/-}$ mice were genotyped by Shanghai Biowing Applied Biotechnology Ltd., using multiplex PCR with next generation sequencing (Chen et al., 2016). All identified SNP were compared with the Mouse Genome Informatics (MGI) database, and were found to be identical with genotype of C57BL/6. The detailed SNP test results were in Table S1 and Table S2 in the supplementary data.

Female $Batf3^{-/-}Apoe^{-/-}$ mice or the $Apoe^{-/-}$ mice were kept on a chow diet (CD) or fed a Western diet (WD) (21% fat and 0.15% cholesterol) (Beijing keaoxieli company, China) for 12 weeks (wks). These mice were 6–8 wks in age, weighed 21–25 g, and were housed at a constant temperature (24 °C) in a 12-hour (h) dark/12-h light-cycle room in the Taishan Medical University Animal Care Facility, according to institutional guidelines. All animal studies were approved by the Animal Care and Utilization Committee of Taishan Medical University.

2.2. Measurements of Atherosclerotic Lesions

For atherosclerotic lesion measurements, the $Apoe^{-/-}$ mice (n = 8) and the $Batf3^{-/-}Apoe^{-/-}$ mice (n = 8) were fed a Western diet for 12 wks, anesthetized using isoflurane, blood was drawn, and the mice were perfused with 2 mmol/L Ethylene Diamine Tetraacetic Acid (EDTA) (Sigma-Aldrich) in Phosphate Buffered Saline (PBS) via cardiac puncture to remove blood contamination from vascular tissue. The aortas were dissected, and the exposed aortas were stained for lipid depositions with Oil Red O (Sigma-Aldrich), and an en face assay was performed (Iqbal et al., 2012). The heart was embedded in OCT compound, and the aortic roots were sectioned into 5 μm slices, generating ~30–40 sections that spanned the entirety of the aortic root, and then stained with Oil Red O (Sigma-Aldrich), hematoxylin and eosin (H&E) or masson-trichrome (Solarbio, Beijing, China). For comparisons of lesion size between the groups, the mean lesion area was quantified from 10 digitally captured sections per mice (Cipriani et al., 2013). For immunohistochemistry detection, cryosections of the aortic root were stained for the presence of leukocytes (CD45), macrophages (Mac3), DCs (CD11c) and T cells (CD3) using specific antibodies to Mac-3 (M3/84; BD Biosciences Cat# 550292, RRID:AB_393587), as well as eBioscience antibodies to CD45.2 (104; eBioscience Cat# 13-0454-85, RRID:AB_466457), CD11c (N418; eBioscience Cat# 13-0114-82, RRID:AB_466363), and CD3 (145-2C11; eBioscience Cat# 13-0031-85, RRID:AB_466320) using standard immunohistochemistry techniques (Subramanian et al., 2013). Images were viewed and captured with a Nikon Labophot 2 microscope equipped with a Spot RT3 colour video camera attached to a computerized imaging system (Nikon corporation, Tokyo, Japan). Quantitative analysis of plaque area was performed by 2 blinded observers using Image-Pro Plus software 6.0 (Media Cybernetics, MD, USA, RRID:SCR_007369). For the immunohistofluorescence analysis, the cryosections were stained with an antibody against CD45 (104; eBioscience Cat# 47-0451-82, RRID:AB_1548781), Mac3 (M3/84; BD Biosciences Cat# 550292, RRID:AB_393587), CCL5 (Bioss Inc. Cat# bs-1324R-Biotin, RRID:AB_11099534). Streptavidin APC-eFluor 780 (eBioscience Cat# 47-4317-82, RRID:AB_10366688) and Goat Rabbit IgG Secondary antibody (Bioss Inc. Cat# bs-0295G-Biotin,RRID:AB_10894308). Images were viewed and captured with a Laser Scanning Confocal Microscope (ANDOR E2V, Leica, Germany).

2.3. Flow Cytometry Analysis

Splenic single-cell suspensions and aortic single-cell suspensions were prepared as described in Supplemental information. Cell surface molecule staining was performed using combinations of specific antibodies to CD45.2 (104; eBioscience Cat# 45-0454-82, RRID:AB_953590), CD11c (N418; eBioscience Cat# 17-0114-82, RRID:AB_469346), IA/IE (M5/114.15.2; BioLegend Cat# 107630, RRID:AB_2069376), CD8a (53-6.7; eBioscience Cat# 95-0081-42, RRID:AB_1603266), CD11b (M1/70; eBioscience Cat# 12-0112-81, RRID:AB_465546), B7-DC (122; eBioscience Cat# 12-9972-82, RRID:AB_466285), B7-H2 (HK5.3; eBioscience Cat# 12-5985-82, RRID:AB_466094), CD40 (1C10; eBioscience Cat# 12-0401-82, RRID:AB_465649), CD80 (16-10A1; eBioscience Cat# 12-0801-82, RRID:AB_465752), CD86 (GL1; eBioscience Cat# 12-0862-83, RRID:AB_465769), CD62L (MEL-14; eBioscience Cat# 12-0621-83, RRID:AB_465722), and CD103 (M290; BD Biosciences Cat# 557493, RRID:AB_396730). For intracellular cytokine staining, splenocytes were prepared as previously described, and were then stimulated with an RPMI-1640 medium containing 10% fetal calf serum (FCS), 20 ng/mL phorbol 12-myristate 13-acetate (PMA) (Sigma-Aldrich), 1 μg/mL ionomycin (Sigma-Aldrich), and 5 μg/mL brefeldin A (selleckchem) for 4 h at 37 °C and 5% CO_2. The cells were washed with washing buffer and then stained with an Anti-Mouse CD4-FITC antibody (GK1.5; eBioscience Cat# 11-0042-86, RRID:AB_46489) or an Anti-Mouse CD8-BV650 antibody (53-6.7; eBioscience Cat# 95-0081-41, RRID:AB_1603267). Then the cells were fixed and permeabilized with a Fixation/Permeabilization Solution (BD Biosciences), and stained intracellularly with Anti-Mouse/Rat IL-17A PerCP-Cyanine5.5 (eBio17B7; eBioscience Cat# 45-7177-80, RRID:AB_925754) and Anti-Mouse IFN-γ APC (XMG1.2; eBioscience Cat# 17-7311-82, RRID:AB_469504) antibodies. Intracellular staining for Foxp3 (FJK-16S; eBioscience Cat# 12-5773-82, RRID:AB_465936) was performed using the Transcription factor staining buffer kit (eBioscience). Flow cytometry analysis was performed using a FACS ARIA II (BD Biosciences) equipped with a 405 nm, 488 nm and a 633 nm laser, and the results were analyzed by FlowJo 7.6 software (Tree Star, OR, USA, RRID:SCR_008520).

2.4. Antigen-specific T Cell Proliferation and Polarization

Naïve $CD4^+CD62L^+$ T cells were sorted from the spleens of OT-II mice by fluorescence-activated cell sorting (FACS) Aria II (BD Biosciences) as shown in Fig. S2a, and labeled with 5 μM cell proliferation

dye eFluor 450 (eBioscience) according to the manufacturers' instructions. CD8α$^+$ DCs and CD8α$^-$ DCs were sorted from the spleens of *Apoe*$^{-/-}$ mice fed either a CD or a WD for 12 wks as shown in Fig. S1b. A co-culture of CD8$^+$ DCs (1×10^4 cells) or CD8$^-$ DCs (1×10^4 cells) with $OVA_{323–339}$ specific CD4$^+$CD62L$^+$ naive T cells (1×10^5 cells) in the presence of 500 ng/mL $OVA_{323–339}$ in RPMI-1640 medium (supplemented with 2 mM L-glutamine, 10% FCS, 100 U/mL penicillin/streptomycin) at 37 °C and 5% CO_2 for four days. The flow cytometric analysis was carried out to quantify T cell proliferation and differentiation by eFluor 450 dye-dilution and intracellular cytokine staining, respectively.

2.5. Quantitative Real-time PCR

Mouse aortic tissues were snap-frozen in liquid nitrogen for RNA extraction with Trizol reagent (Takara). RNA of the FACS-based purified aortic CD45$^+$ leukocytes or CD45$^-$ non-leukocytes and splenic macrophages, CD8α$^+$ DCs or CD8α$^-$ DCs were extracted using an RNAprep Pure Micro Kit (Tiangen Biotech company, Beijing, China). RNA that was extracted from the aorta and cells were subjected to reverse transcription using FastQuant RT Kit (with gDNase) (Tiangen company, Beijing, China). The samples subsequently underwent quantitative real-time polymerase chain reaction (qPCR) using SYBR Green (Qiagen, Germany) with the use of Qiagen real-time PCR system (Qiagen, Rotor-Gene Q, Germany). Gene-specific intron-spanning primers were designed with Primer-BLAST (NCBI). For validation of primer specificity, nucleotide blast specificity analysis was performed. Primer sequences were listed in (Table S3). Relative gene expression was normalized to Glyceraldehyde 3-phosphate dehydrogenase (*Gapdh*) as an internal control, and was performed using the ΔΔCt method, as previously described (Schmittgen and Livak, 2008).

2.6. Enzyme-linked Immunosorbent Assay (ELISA)

Aortic tissue ELISA were performed as we previously described (He et al., 2016). Briefly, after cardiac perfusion, the mouse aorta tissues was removed and weighed. Following homogenization with homogenizor (OPTIMA INC, Japan) and lysation by 500 μL of Radio-Immunoprecipitation Assay (RIPA) Buffer (Cell Signaling Technology, Inc) per aorta, proteins from aorta were extracted after centrifugation, and then quantified by bicinchoninic acid (BCA) protein quantization kits (Solarbio, Beijing, China). The concentration of IL-12 P70, IFN-γ and CCL5 in the aorta or the IFN-γ in the plasma was detected using commercial ELISA kits (all the kits were purchased from eBioscience) according to the manufacturers' instructions. Results were shown as concentration of cytokines or chemokine per gram of aortic total protein. IL-12 p70 protein levels were quantified in the cell culture supernatants using a murine IL-12p70 ELISA kit (eBioscience) according to the manufacturer's instructions. All ELISA detection was performed using a plate reader (Tecan, Infinite M200 Pro, Switzerland).

2.7. Primary Splenic Macrophages Sorting and Treatment

The spleen cells from C57BL/6 J mice were prepared, then the primary macrophages were sorted as described in supplementary data, then cultured with 100 ng/mL IFN-γ (Peprotech, NJ, USA) in RPMI1640 10% culture medium for 6 h in a 37 °C humidified incubator containing 5% CO_2.

2.8. Statistical Analysis

Unpaired Student *t*-tests were used to analyze the data, and if there were more than two groups, the data were analyzed by a one-way ANOVA. Differences of $P < 0.05$ were considered to be statistically significant. Data was processed using GraphPad Prism 6.0 software (La Jolla, CA, USA, RRID:SCR_002798).

3. Results

3.1. Ablation of CD8α$^+$ DCs in *Batf3*$^{-/-}$*Apoe*$^{-/-}$ Mice Alleviates Atherosclerosis

To evaluate the role of CD8α$^+$ DCs in atherosclerotic plaque formation, double knockout for *Batf3*$^{-/-}$*Apoe*$^{-/-}$ mice was created. After 12 wks of a WD, single cells suspension was prepared from the spleen or the aorta of the *Apoe*$^{-/-}$ control and *Batf3*$^{-/-}$*Apoe*$^{-/-}$ mice. As shown in Fig. 1a, compared with the *Apoe*$^{-/-}$ control mice, the *Batf3*$^{-/-}$ *Apoe*$^{-/-}$ mice displayed a significant decrease of CD8α$^+$ DCs in the spleen ($P < 0.001$) (Fig. 1a), and the CD103$^+$ DCs in the aorta ($P < 0.001$) (Fig. 1a). Since Non-lymphoid tissue-derived CD103$^+$ dendritic cells (DCs) form a unified subset developmentally related to CD8α$^+$ conventional dendritic cells (cDCs) that resided in lymphoid tissues (Edelson et al., 2010), and both of their development are dependent on transcription factor Batf3. These data demonstrate that in *Batf3*$^{-/-}$*Apoe*$^{-/-}$ mice, both CD8α$^+$ DCs and CD103$^+$ DCs are effectively depleted, even under WD conditions.

To investigate the impact of CD8α$^+$ DCs depletion on atherosclerotic plaque formation, we analyzed atherosclerosis lesions after 12 wks of being fed a WD. We observed that the atherosclerosis lesion area in the aortic root was significantly alleviated (Fig. 1b). To further confirm this, an en face staining analysis was also performed. As shown in Fig. 1c, we found that the oil red area of the aorta of *Batf3*$^{-/-}$*Apoe*$^{-/-}$ mice was significantly reduced (Fig. 1c). We also analyzed plaque collagen content by masson-trichrome staining, and observed the collagen content in *Batf3*$^{-/-}$*Apoe*$^{-/-}$ mice to be significantly increased (Fig. S1), which was indicated a more stable plaque. These data effectively demonstrate that depleting CD8α$^+$ DCs in the spleen or CD103$^+$ DCs in the aorta result in alleviation of atherosclerosis.

It is well known that atherosclerosis is closely associated with plasma lipids, blood glucose, and body weight (Iqbal et al., 2012). Moreover, the potential ability of DCs to regulate plasma lipids has also recently been recognized (Rolin and Maghazachi, 2014). To examine whether the plasma lipids, blood glucose, and body weight were altered in WD-treated *Batf3*$^{-/-}$*Apoe*$^{-/-}$ mice, these mice were fed a WD for 12 wks. Compared with the *Apoe*$^{-/-}$ mice, no changes in plasma total cholesterol (TC), triglycerides (TG), high-density lipoprotein (HDL), and low-density lipoprotein (LDL) from *Batf3*$^{-/-}$ *Apoe*$^{-/-}$ mice were detected (Fig. S2a). The liver function of *Batf3*$^{-/-}$*Apoe*$^{-/-}$ mice also remained unchanged, as the level of alanine aminotransferase (ALT) in the plasma was comparable with that of control mice (Fig. S2b). Plasma glucose (Fig. S2c) and body weight did not have any significant differences between the two groups (Fig. S2c, d). These findings indicate that the plasma lipid levels and blood glucose were not the cause of alleviating atherosclerosis due to depletion of CD8α$^+$ DCs.

3.2. Ablation of CD8α$^+$ DCs Decreased Th1 Cells but not Th17 Cells and Treg Cells Populations in the Spleen

Given that various T cell subsets (e.g., Th1 cells, Th17 cells, and Treg cells) play essential roles in the regulation of atherogenesis (Benagiano et al., 2003; Smith et al., 2010; Subramanian et al., 2013), and distinct DC subsets are critical for the induction of different types of CD4$^+$ T helper responses, we next sought to examine whether the type of T cell response in the spleens of *Batf3*$^{-/-}$*Apoe*$^{-/-}$ mice was altered. The flow cytometry analysis revealed that there was a significant decrease in the proportion of CD4$^+$IFN-γ$^+$ Th1 cells in the spleens of *Batf3*$^{-/-}$ *Apoe*$^{-/}$ -mice (Fig. 2a). However, there were no changes in the total splenic cell numbers (data not shown) under WD conditions, and no significant difference was found in the number of Th17 cells and Treg cells (Fig. 2b). We did not detect Th2 cells here as hardly any report showing the role of Th2 cells in atherosclerosis. Since the dominant role of CD8α$^+$ DCs in cross-presentation is well-established (Busche

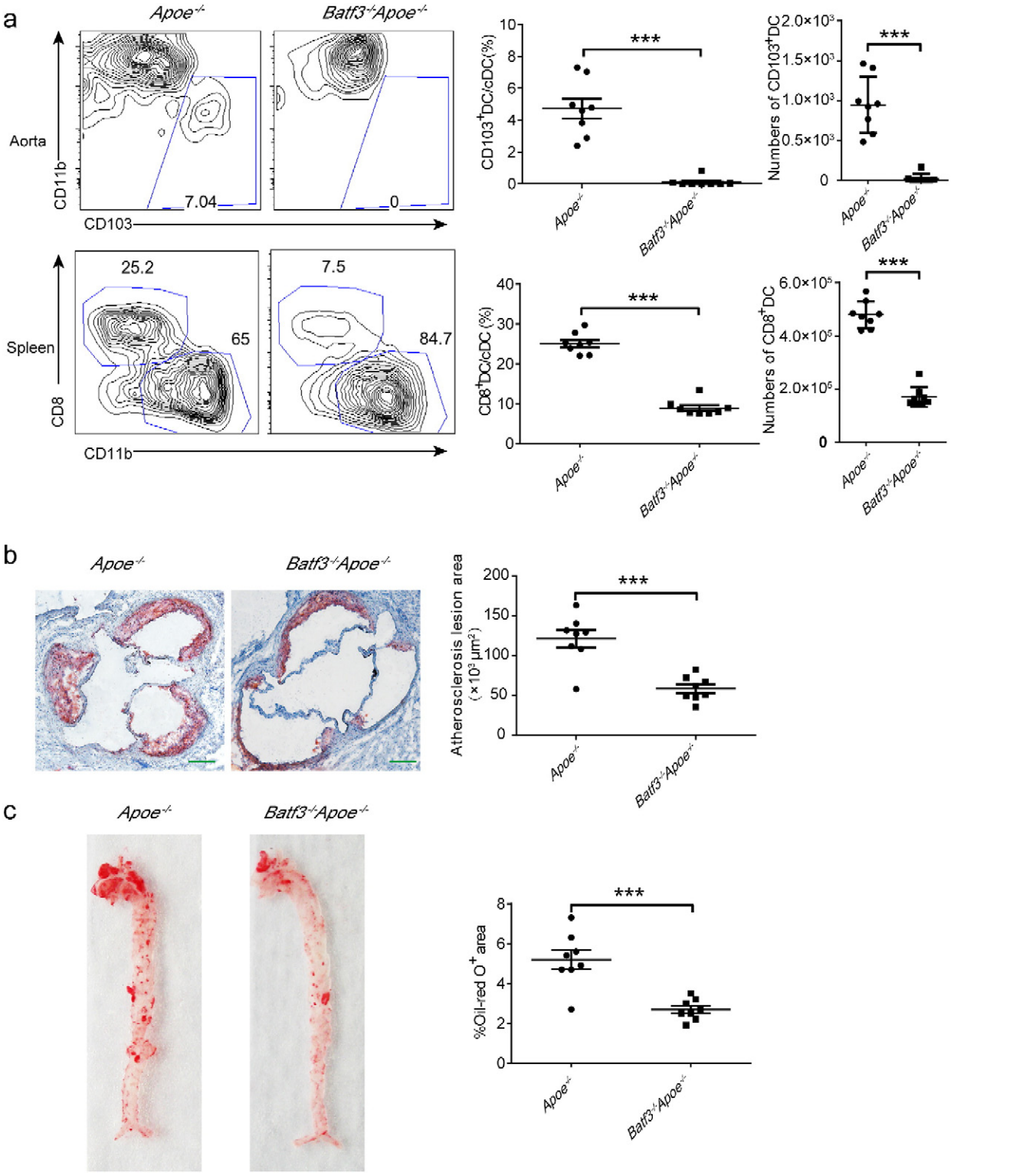

Fig. 1. *Batf3* deficiency effectively depleted CD8α$^+$ DCs in the spleen and CD103$^+$ DCs in the aorta, and alleviated atherosclerosis in *Apoe*$^{-/-}$ mice. The *Apoe*$^{-/-}$ mice (n = 8) and the *Batf3*$^{-/-}$*Apoe*$^{-/-}$ mice(n = 8)were fed a WD for 12 weeks. (a) The single cell suspensions of the spleen and aorta were prepared, the proportion and the cells number of CD8α$^+$ DCs in the spleen or CD103$^+$ DCs in the aorta was detected by flow cytometry. (b) Cryosections of the aortic root were performed Oil Red O staining to quantify the lesion area. Scale bars: 200 μm. (c) Aorta en face staining of Oil Red O. Representative images of the aortic root. Data are presented as mean ± SD. Differences of $P < 0.05$ were considered to be statistically significant. ***$P < 0.001$; ns, not significant. Data are representative of three independent experiments. See also Fig. S1 and S2.

et al., 2013), we next investigated whether CD8α$^+$ DCs ablation also impact IFN-γ secretion by CD8$^+$T cells. Consistent with our hypothesis, we found that IFN-γ secretion was decreased by CD8$^+$T cells in the spleens of *Batf3*$^{-/-}$*Apoe*$^{-/-}$ mice (Fig. S3). Therefore, we concluded that CD8α$^+$ DCs selectively induce a CD4$^+$Th1 cell response and also induce IFN-γ secretion by CD8$^+$T cells. However, they do not modulate the Th17 cells and Treg cells during atherosclerosis development. Furthermore, the plasma IFN-γ was detected using ELISA. Our data showed

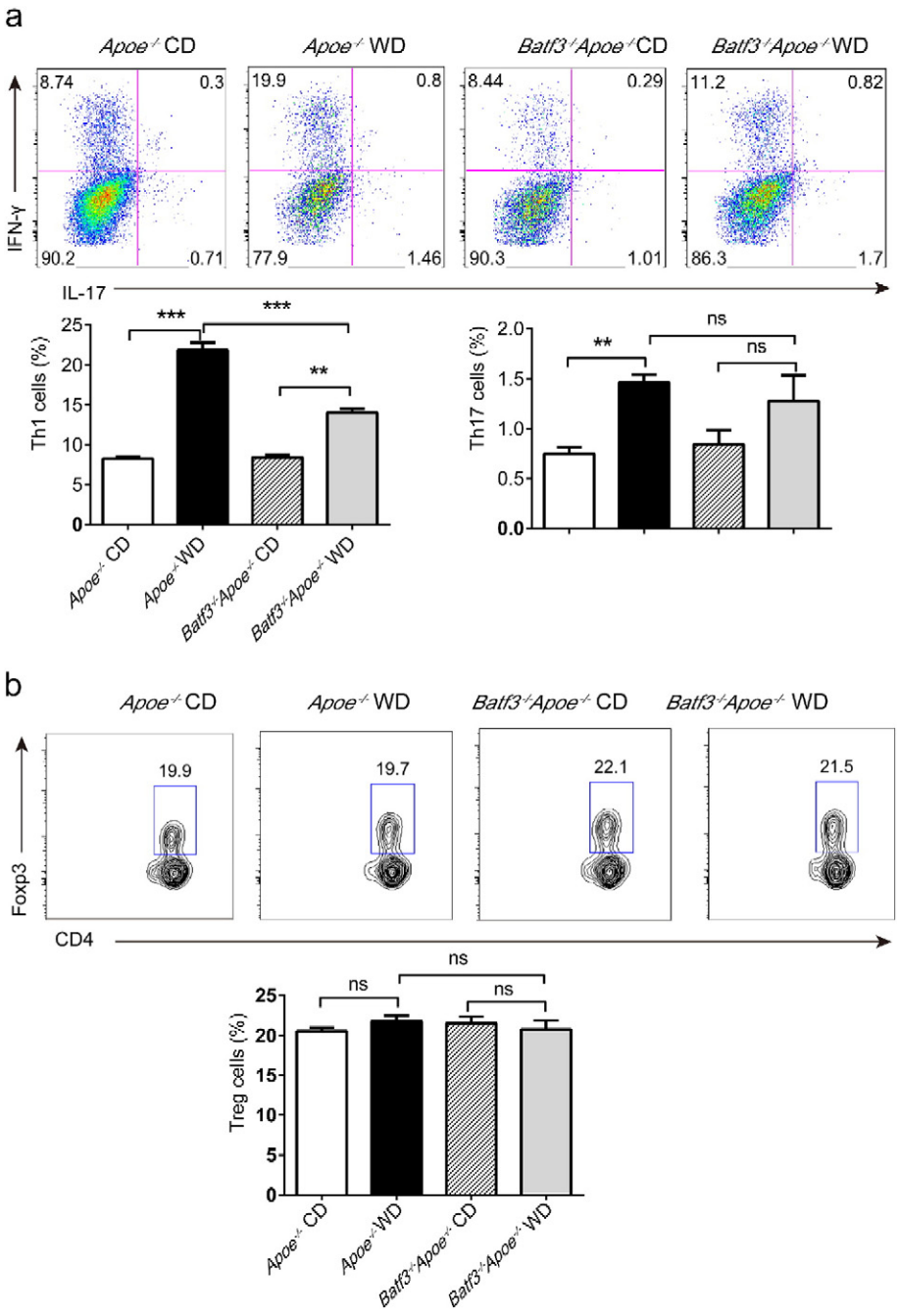

Fig. 2. Ablation of CD8α$^+$ DCs induces decreased Th1 cells but not Th17 cells and Treg cells responses in the spleen. (a) Flow cytometry analysis of the spleen CD4$^+$IFN-γ$^+$ (Th1) cells and CD4$^+$IL-17$^+$ (Th17) cells. The *Apoe*$^{-/-}$ mice (n = 8) and the *Batf3*$^{-/-}$*Apoe*$^{-/-}$ mice (n = 8) were fed either a chow diet or Western diet for 12 weeks. The splenocytes were stimulated with PMA (20 ng/mL), ionomycin (1 μg/mL), and Brefeldin A (5 μg/mL), at 37 °C, 5% CO_2 for 4 h, and then assayed for assessment of Th1 cell and Th17 cell responses by flow cytometry. (b) Flow cytometry analysis of the spleen CD4$^+$Foxp3$^+$Tregs. Intracellular staining was performed on splenocytes for foxp3 detection using the Transcription factor staining buffer set according to the manufacturers' instructions. Data are presented as mean ± SD. Differences of $P < 0.05$ were considered to be statistically significant. $^{**}P < 0.01$; $^{***}P < 0.001$; ns, not significant. Data are representative of three independent experiments. See also Fig. S3.

that the plasma IFN-γ decreased in *Batf3*$^{-/-}$*Apoe*$^{-/-}$ mice when compared with the *Apoe*$^{-/-}$ mice (Fig. S3c), which was consistent with the decreased Th1 cell response and IFN-γ secretion by CD8$^+$T displayed in *Batf3*$^{-/-}$*Apoe*$^{-/-}$ mice (Fig. 2a, S3a and b).

3.3. CD8α$^+$ DCs from *Apoe*$^{-/-}$ Mice Fed a Western Diet, Induced an Increase in T Cell Proliferation and Th1 Cell Differentiation In Vitro

To further confirm the observation that CD8α$^+$ DCs induced the Th1 cell response under the conditions of a WD, we sorted and cocultured splenic CD8α$^+$ DCs or CD8α$^-$ DCs from CD-treated mice or WD-treated mice with naïve OT-II T cells from OVA-specific TCR transgenic OT-II mice in the presence of an $OVA_{323-339}$ peptide. As shown in Fig. S4 and Fig. 3a, splenic CD8α$^+$ DCs isolated from mice fed a WD (CD8+/WD), induced more substantial proliferation of OT-II T cells compared to CD fed mice according to the split peak of eFluor 450. However, there was no significant difference in the induction of T cell proliferation between CD8α$^-$ DCs from mice fed a CD (CD8−/CD) and CD8α$^-$ DCs fed a WD (CD8−/WD) (Fig. 3a). In inducing Th1 cell differentiation, we found that at the basic level, CD8a$^-$DCs are more potent than CD8a$^+$DCs to induce Th1 cells in vitro. But when compared with CD-treated mice, only CD8a$^+$ DCs but not CD8a$^-$ DCs derived from WD-

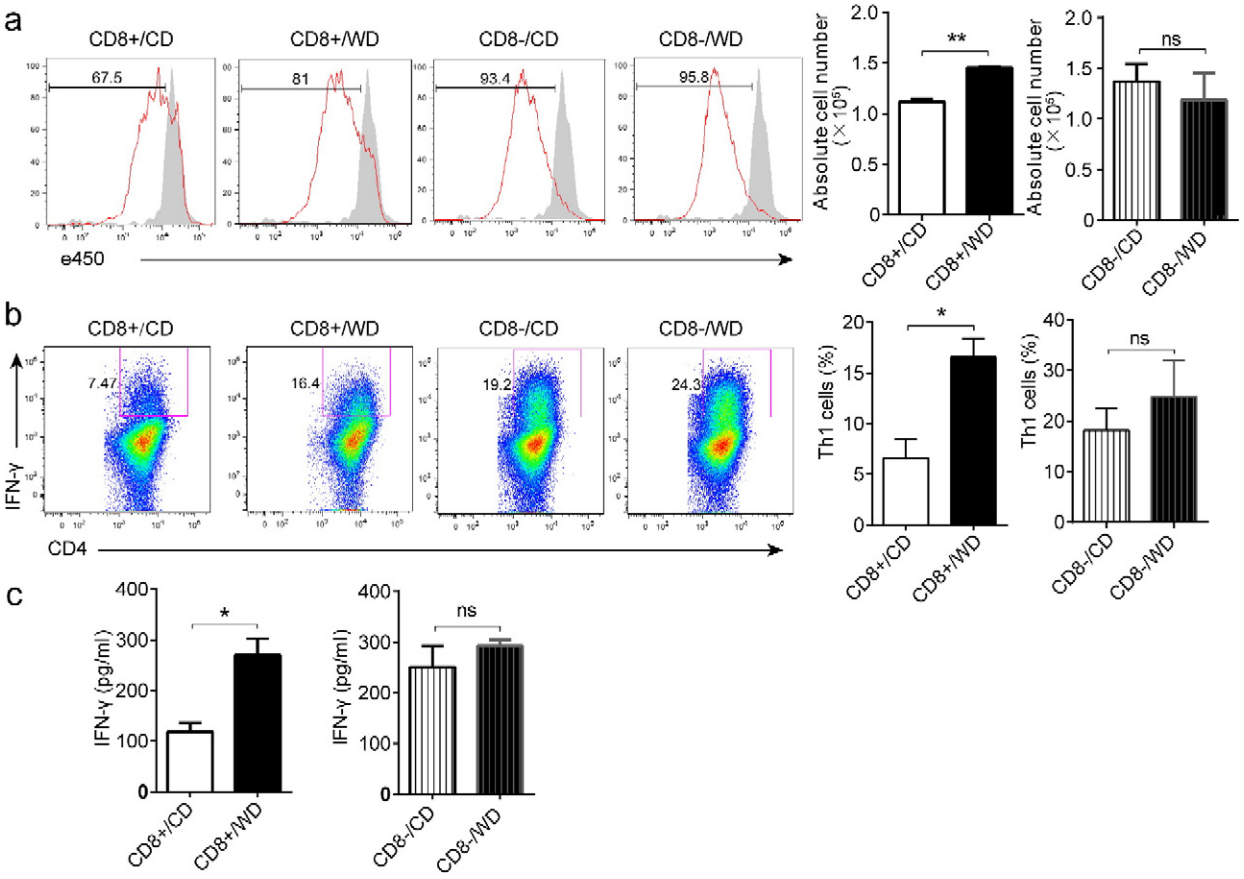

Fig. 3. CD8α$^+$ DCs from *Apoe*$^{-/-}$ mice fed a western diet preferentially induced Th1 cell differentiation in vitro. (a) Flow cytometry analysis of a coculture of DC subsets as indicated, and eFluor 450 labeled naïve CD4$^+$T cell in the presence of $OVA_{323-339}$ (500 ng/mL), four days after coculture. e450 dilution peaks of the CD4$^+$T cells were analyzed. (b) Coculture of DC subsets as denoted, and naïve CD4$^+$T cells in the presence of $OVA_{323-339}$ peptide (500 ng/mL). Four days after coculture, Th1 cell polarization was analyzed by intracellular cytokine (ICC) staining and then by Flow cytometry analysis. (c) ELISA analysis of the IFN-γ content from the cocultured supernatants. A volume of 100 μL from supernatants was used to detect the IFN-γ content using an IFN-γ ELISA kit (eBioscience) according to the manufacturers' instructions. Data are presented as the mean ± SD. Differences of $P < 0.05$ are considered to be statistically significant. *$P < 0.05$; **$P < 0.01$; ns, not significant. Data are representative of three independent experiments. See also Fig. S4.

treated mice could promote Th1 cell differentiation (Fig. 3b, c). That is to say, increased Th1 cells under WD condition were not associated with CD8a$^-$ DCs. These data were also consistent with reports that high-fat/cholesterol diet-induced dyslipidemia, where CD8α$^-$ DCs preferentially induce a Th2 response (Shamshiev et al., 2007). Together, these data demonstrate that CD8α$^+$ DCs from *Apoe*$^{-/-}$ mice fed a WD preferentially induced Th1 cell differentiation in vitro, which was consistent with the data shown in Fig. 2.

3.4. CD8α$^+$ DCs From the Spleen of Mice Fed a Western Diet Expressed Higher Levels of CD86 and IL-12

To gain insight into the potential mechanisms by which CD8α$^+$ DCs from *Apoe*$^{-/-}$ mice fed a WD, preferentially induced Th1 cell differentiation in vivo, we first performed qPCR analysis using splenic DCs isolated from *Apoe*$^{-/-}$ mice. By analyzing certain critical surface molecules linked to inducing T cell proliferation and Th1 cell differentiation, we found that DCs from the CD8 +/WD group expressed higher levels of *Cd86* than the CD8 +/CD group (Fig. 4a). This was further confirmed by flow cytometry (Fig. 4b). In CD8α$^-$ DCs, although CD8 −/WD group expressed higher levels of *Cd86* than the CD8 −/CD group by flow cytometry (Fig. S5b), however *Cd70* expression decreased (Fig. S5a). Perhaps, together with other undetected molecule, CD8 −/WD didn't induce increased CD4$^+$T cells proliferation. These data indicate that CD86 is associated with CD8α$^+$ DCs induced increased CD4$^+$T cells proliferation under the conditions of a WD. Since IL-12p70 is a key cytokine secreted by DCs to polarize Th1 cell differentiation (Vignali and Kuchroo, 2012), we measured IL-12p70 expression in CD8α$^+$ DCs. As expected, CD8α$^+$ DCs from WD-treated mice produce higher levels of *Il12a* (a subunit of IL-12p70) as analyzed by qPCR (Fig. 4a) and confirmed by ELISA (Fig. 4c). These results indicate that splenic CD8α$^+$ DCs from the CD8 +/WD group produced higher levels of IL-12 than the CD8 +/CD to trigger Th1 cell polarization. Although some reports have shown that CD36 was related to uptake of lipids by DCs and contribution to atherosclerosis (Stewart et al., 2010), and CD70 was related to Th1 cell differentiation (Soares et al., 2007). However, no alteration of these two molecules was noted (Fig. 4a). Interestingly, in CD8α$^-$ DCs, there was no difference between CD8 −/CD and CD8 −/WD in *Il12* and *Cd36* expression (Fig. 5Sa, b). Together, these data suggest that splenic CD8α$^+$ DCs from mice fed a WD, induce Th1 cell differentiation dependent on IL-12, but independent of CD70 or CD36. These data were consistent with reports that CD8α$^+$ DCs are source of IL-12 to mount protective Th1 type immunity against the parasitic infection (Ashok et al., 2014; Mashayekhi et al., 2011).

3.5. Ablation of CD8α$^+$ DCs Led to a Decrease in IFN-γ and CCL5 Expression in the Aorta

To further investigate the impact of CD8α$^+$ DC ablation on the local aortic Th1 cells-related immune response, we further analyzed the aortic cytokines and transcription factors associated with differential T cell subsets, and found a significant decrease in the aortic *Ifng* mRNA expression (Fig. 5a). These results were then further confirmed by ELISA (Fig. 5b). Consistent with these results, T-bet (gene name *Tbx21*), the key

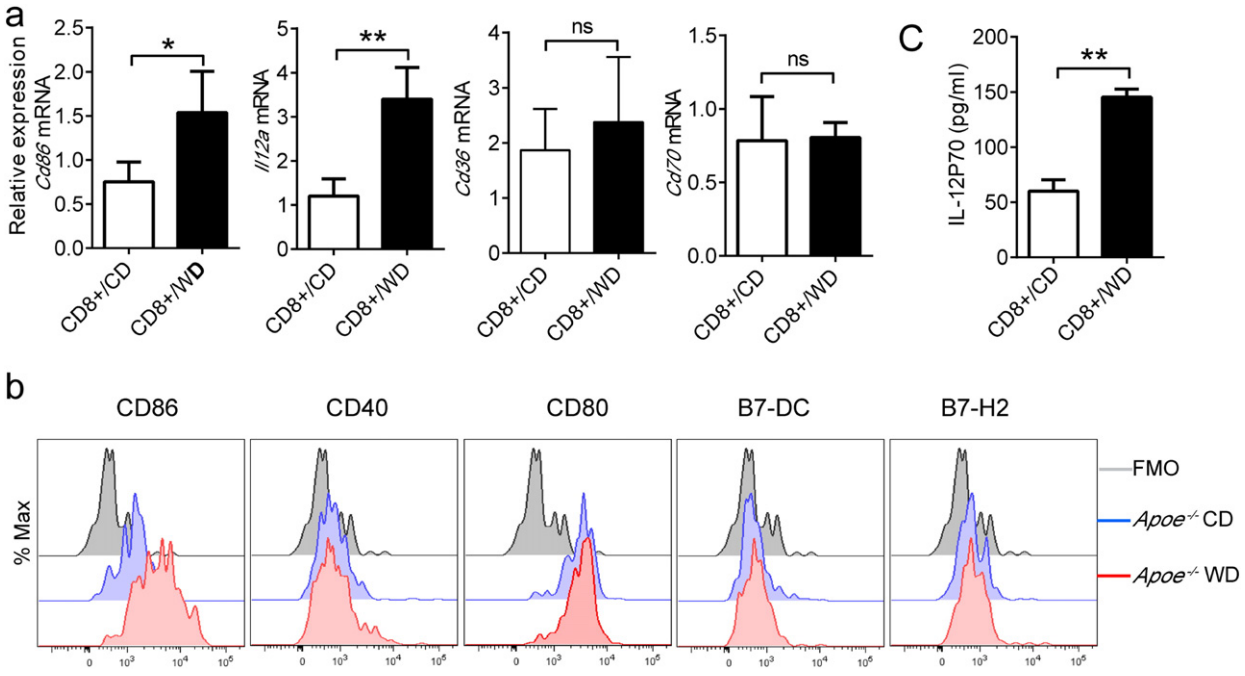

Fig. 4. CD8α$^+$ DCs expressed higher levels of CD86 and IL-12p35 with the WD. The *Apoe*$^{-/-}$ mice were fed on a chow diet (*Apoe*$^{-/-}$CD, n = 8) or a western diet (*Apoe*$^{-/-}$WD, n = 8) for 12 weeks, and the splenocytes were used for analysis. (a) CD8α$^+$ DCs from the chow diet(CD8 + /CD) and western diet(CD8 + /WD)were sorted from the spleen as described previously by FACS, the RNA was extracted, and *Cd86*, *Il12a*, *Cd36* and *Cd70* mRNA expression was analyzed by qPCR (data are represented normalized to *Gapdh* and relative to the CD8 + /CD control). (b) Flow cytometry analysis of mean fluorescent intensity (MFI) of CD8α$^+$ DCs surface markers CD86, CD40, CD80, B7-DC, and B7-H2. Gray solid area, fluorescent minus one (FMO) staining control. (c) IL-12p70 in the cocultured supernatants of CD8α$^+$ DCs and naïve CD4$^+$CD62L$^+$T by ELISA. Sorted splenic CD8α$^+$ DCs from the CD8 + /CD or CD8 + WD group was cocultured with naïve CD4$^+$CD62L$^+$ T cells as described above, and 100 μL supernatants were used to detect the IL-12p70 content using an IL-12p70 ELISA kit (eBioscience). Data are presented as the mean ± SD. Differences of a $P < 0.05$ were considered to be statistically significant. $^*P < 0.05$; $^{**}P < 0.01$; ns, not significant. Data are representative of three independent experiments. See also Fig. S5.

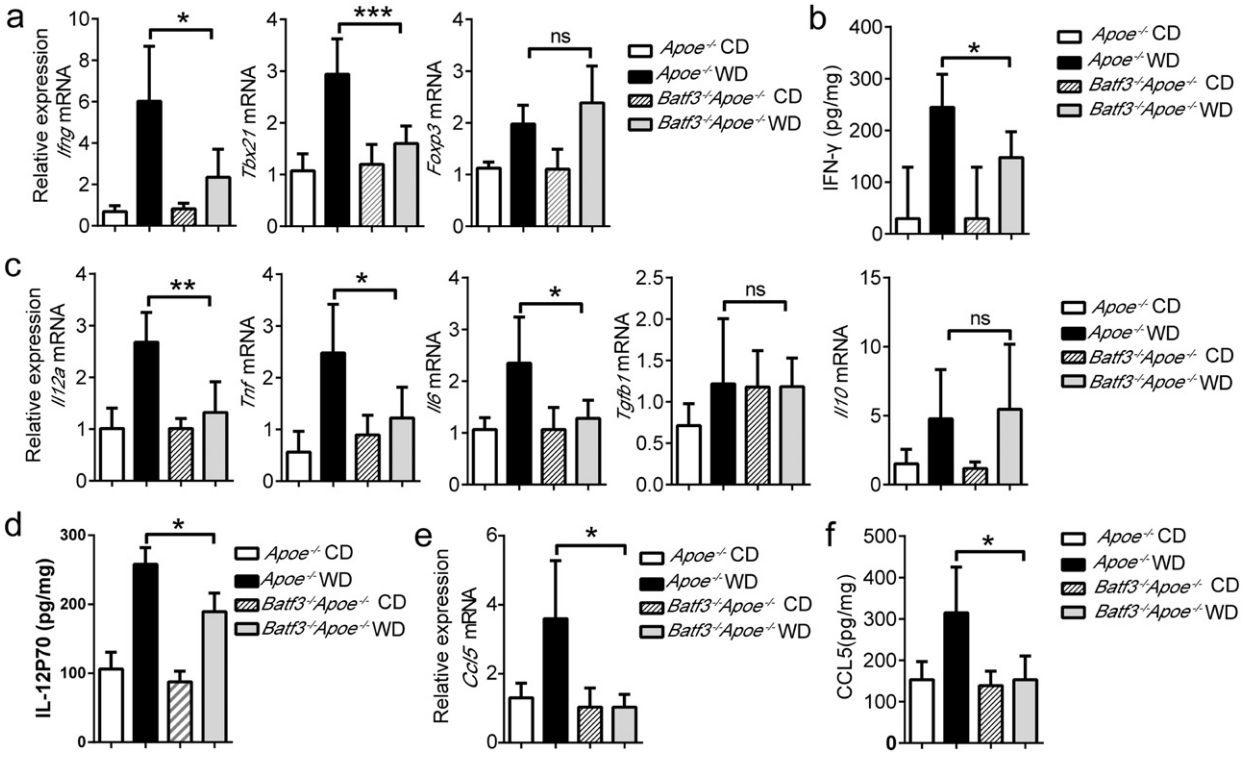

Fig. 5. Lack of CD8α$^+$ DCs led to decreased IFN-γ and CCL5 expression in the aorta. The *Apoe*$^{-/-}$ mice (n = 8) and the *Batf3*$^{-/-}$*Apoe*$^{-/-}$ mice (n = 8) were fed either a chow diet or Western diet for 12 weeks. (a) Analysis of aortic *Ifng*, *Foxp3*, and *Tbx21* mRNA expression by qPCR. (b) An aortic tissue ELISA analysis of IFN-γ. Data represent pg/mg aortic protein. (c) qPCR analysis of *Il12a*, *Tnf*, *Il6*, *Tgfb1*, and *Il10*mRNA expression. (d) qPCR analysis of *Ccl5* expression. (e) ELISA analysis of the CCL5 concentration in the aortic tissue. Data represent pg per mg aortic protein. Data are presented as mean ± SD. Differences of a $P < 0.05$ were considered to be statistically significant. $^*P < 0.05$; $^{**}P < 0.01$; $^{***}P < 0.001$; ns, not significant. Data are representative of three independent experiments. See also Fig. S6.

transcription factor required for Th1 cell differentiation was significantly decreased, however the transcription factor, *Foxp3* required for Treg cells was unaltered (Fig. 5b). These data indicated that the aortic local T cell polarization was similar to the spleen. Furthermore, IL-12, a cytokine preferentially produced by CD8α$^+$ DCs (Huang et al., 2001) and essential for DC-mediated Th1 cell differentiation, was significantly decreased (Fig. 5c, d). Although *Il6* was decreased, no alterations in the levels of Transforming growth factor beta 1 (*Tgfb1*) and *Il10* (Fig. 5c) were observed. This indicates that the local Treg cells and Th17 cells were not likely involved in the local inflammation of CD8α$^+$ DC-depleted *Apoe*$^{-/-}$ mice. Interestingly, the reduction in the proinflammatory cytokines, tumor necrosis factor (TNF)-α (gene name *Tnf*), *Il6*, and *Il12* denote the reduced aortic inflammation with the ablation of CD8α$^+$ DCs. These data further demonstrated that the depletion of CD8α$^+$ DCs led to a decreased Th1 cell response and inflammation in the aorta.

IFN-γ signaling has many downstream target genes potentially relevant to atherosclerosis, particularly those encoding various chemokines (Millward et al., 2007; Wuttge et al., 2004). Several reports suggest that during inflammatory conditions, IFN-γ can induce chemokine production (Kawka et al., 2014; Millward et al., 2007; Schroder et al., 2004). Therefore, we hypothesized that decreased IFN-γ production due to CD8α$^+$ DC ablation could affect the expression of IFN-γ-dependent chemokines in atherosclerosis. Although we did not observe down-regulation in *Ccl2*, *Ccl17*, vascuolar cell adhesion molecule-1 (*Vcam1*), *Cx3cl1*, *Cxcl1*, *Cxcl4*, *Cxcl10*, *Cxcl11*, *Cxcl12*, and *Cxcl16* (Combadiere et al., 2008; Heller et al., 2006; Weber et al., 2011; Wuttge et al., 2004) (Fig. S6a), we found a significant decrease in *Ccl5* mRNA levels in the aorta. Further detection of the CCL5 levels by ELISA confirmed this result (Fig. 5e). CCL5 is known to bind to several receptors (e.g., CCR1, CCR3, and CCR5) (Suffee et al., 2012), however, no alterations in these receptors were detected (Fig. S6b). Taken together, these data indicate that ablation of CD8α$^+$ DCs resulted in a reduced Th1 cell response, attenuated CCL5 expression, and alleviated inflammation in the aorta.

3.6. IFN-γ Promoted CCL5 Expression in Macrophages, Which May Enhance Infiltrating Leukocytes into Atherosclerotic Plaques

CCL5 has been previously shown to promote the recruitment of leukocytes into atherosclerotic aortas (Braunersreuther et al., 2008), and the enhanced infiltration of these cells into the lesions and arterial wall is associated with an acceleration of the disease. However, there are potentially no direct correlations between CD8α$^+$ DCs and CCL5 in the progression of atherosclerosis according to published studies. We hypothesized that CD8α$^+$ DCs potentially promote CCL5 expression in the atherosclerotic aorta via polarization of IFN-γ producing Th1 cells, since the potential role of IFN-γ in modulating CCL5 expression is well-established (Liu et al., 2005).

To address this, we next sought to examine the source of CCL5 in the aortic atherosclerotic lesion area. We found that *Ccl5* was primarily expressed in aortic CD45$^+$ leukocytes by both qPCR analysis (Fig. 6a and S7) and immunofluorescent staining (Fig. 6b). Furthermore, using an immunofluorescence staining assay, we found that most of the CCL5 positive signals were colocalized with MAC3 (a macrophages marker) (Braunersreuther et al., 2008; Wang et al., 2014). This suggests that aortic macrophages were the major CCL5-expressing leukocytes in atherosclerotic plaques (Fig. 6c). This result was consistent with a previous study (Tabas and Bornfeldt, 2016; Veillard et al., 2004). Importantly, the ratio of CCL5$^+$ MAC3$^+$ double positive cells was markedly decreased in the aortic plaque of *Batf3*$^{-/-}$*Apoe*$^{-/-}$ mice (Fig. 6c). These data strongly indicate that aortic macrophages were the major source of CCL5 in atherosclerotic aortas, and that their CCL5 expression was modulated by CD8α$^+$ DCs.

Next, we sought to determine whether IFN-γ could promote CCL5 expression on macrophages in an atherosclerosis-related setting. Since there were limited aortic macrophages for further study, we sorted the primary splenic macrophages as previously described (Xu et al., 2016). Interestingly, we found that IFN-γ promoted CCL5 expression on primary macrophages (Fig. 6d), which is consistent with the link between CCL5 and IFN-γ in vivo (Figs. 5, 6c).

CCL5 is closely related to leukocyte chemotaxis, and it has been reported that CCL5 antagonist treatment could inhibit the recruitment of T cells and macrophages into the plaque area, and thus alleviate atherosclerosis (Braunersreuther et al., 2008). We speculated that the reduced CCL5 expression in atherosclerotic plaques of CD8α$^+$ DCs-depleted mice could result in the decreased infiltration of these cells into the plaque. Indeed, the infiltrating cells in the atherosclerotic plaque of *Batf3*$^{-/-}$*Apoe*$^{-/-}$ mice were significantly decreased as analyzed by H&E staining (Fig. 6e). Moreover, further immunohistochemistry staining revealed that leukocytes (e.g., macrophages, DCs, and T lymphocytes) were significantly decreased in the aortic plaque (Fig. 6f), while no changes were observed in the smooth muscle cells (data not shown).

Collectively, our data demonstrate an important role of Batf3-dependent CD8α$^+$ DCs in controlling IFN-γ production and IFN-γ-dependent CCL5 expression by macrophages during atherosclerotic progression. The absence of CD8α$^+$ DC-dependent enhancement of CCL5 expression likely explains the decreased aortic accumulation of inflammatory leukocytes, including macrophages, T cells, and DCs.

4. Discussion

The role of DCs in modulating immune responses involving atherogenesis has been suggested previously (Choi et al., 2011; Gautier et al., 2009). However, the role of CD8α$^+$ DCs in atherogenesis remains elusive. Non-lymphoid tissue-derived CD103$^+$ dendritic cells (DCs) form a unified subset developmentally related to CD8α$^+$ conventional dendritic cells (cDCs) that resided in lymphoid tissues. The relationship between CD8$^+$ cDCs and CD103$^+$ DCs implied by their shared dependence on transcription factor Batf3 and Irf8 was further supported by similar patterns of gene expression. These data provided evidence for a developmental relationship between lymphoid organ–resident CD8$^+$ cDCs and non-lymphoid tissue-derived CD103$^+$ DCs (Edelson et al., 2010). One study using *Flt3*$^{-/-}$ *Ldlr*$^{-/-}$ double deficient mice suggested that aortic CD103$^+$ DCs promote Treg cells responses and inhibit atherosclerosis (Choi et al., 2011). In contrast, our results indicate that CD8α$^+$ DCs promote atherosclerosis by preferentially inducing IFN-γ-producing Th1 cells and IFN-γ-producing CD8$^+$T cells. These cells in turn, promote immune cell accumulation in atherosclerotic plaque via activation of plaque macrophages to secrete CCL5. A potential explanation for these differences between our results and previous studies could be due to the following reasons: 1) since flt3 is a key cytokine for the development of conventional DCs (CD8α$^+$ DCs and CD11b$^+$ DCs) and plasmacytoid dendritic cells (pDCs), in the absence of flt3 signaling, none of the DC subsets could be generated. Therefore, it is unlikely that *Flt3*$^{-/-}$ *Ldlr*$^{-/-}$ double-deficient mice are a suitable model for evaluating the role of CD8α$^+$ DCs or CD103$^+$ DCs in atherosclerosis; and 2) it has been demonstrated that there are intrinsic homeostatic feedback mechanisms between DCs and Treg cells, as decreasing the number of DCs by genetic deletion of Flt3L or by the administration of flt inhibitors leads to a decrease in the number of regulatory T cells (Liu and Nussenzweig, 2010). This indicates that the number of Treg cells in *Ldlr*$^{-/-}$ and *Flt3*$^{-/-}$ *Ldlr*$^{-/-}$ mice might be different under steady-state conditions. It is unlikely that the reduced Treg cells in flt3$^{-/-}$ ldlr$^{-/-}$ mice fed a WD were solely caused by the lack of CD8α$^+$ DCs or CD103$^+$ DCs. In addition, since the number of Treg cells were not declined in *Batf3*$^{-/-}$ mice (Leventhal et al., 2016), confirmed by our results, it is highly likely that another DC subset (e.g., CD11b$^+$DCs) might be involved in the homeostatic maintenance of Treg cells (Weber et al., 2011), instead of CD8α$^+$ DCs. However, further investigation is required. Another recent study used *Batf3*$^{-/-}$chimeras, in which lethally irradiated *Ldlr*$^{-/-}$ mice were reconstituted with bone marrow from *Batf3*$^{-/-}$ mice. This study showed that loss of CD8α$^+$ DCs in

hyperlipidemic mice profoundly reduced cross-priming ability, nevertheless it did not influence lesion development (Legein et al., 2015). Different from the previous study, we used another strategy to prepare *Batf3*$^{-/-}$*Apoe*$^{-/-}$ mice through hybridization of *Apoe*$^{-/-}$ mice and *Batf3*$^{-/-}$ mice. Interestingly, we identified a critical role where Batf3-dependent CD8α^{+} DC aggravated atherosclerosis by inducing a Th1

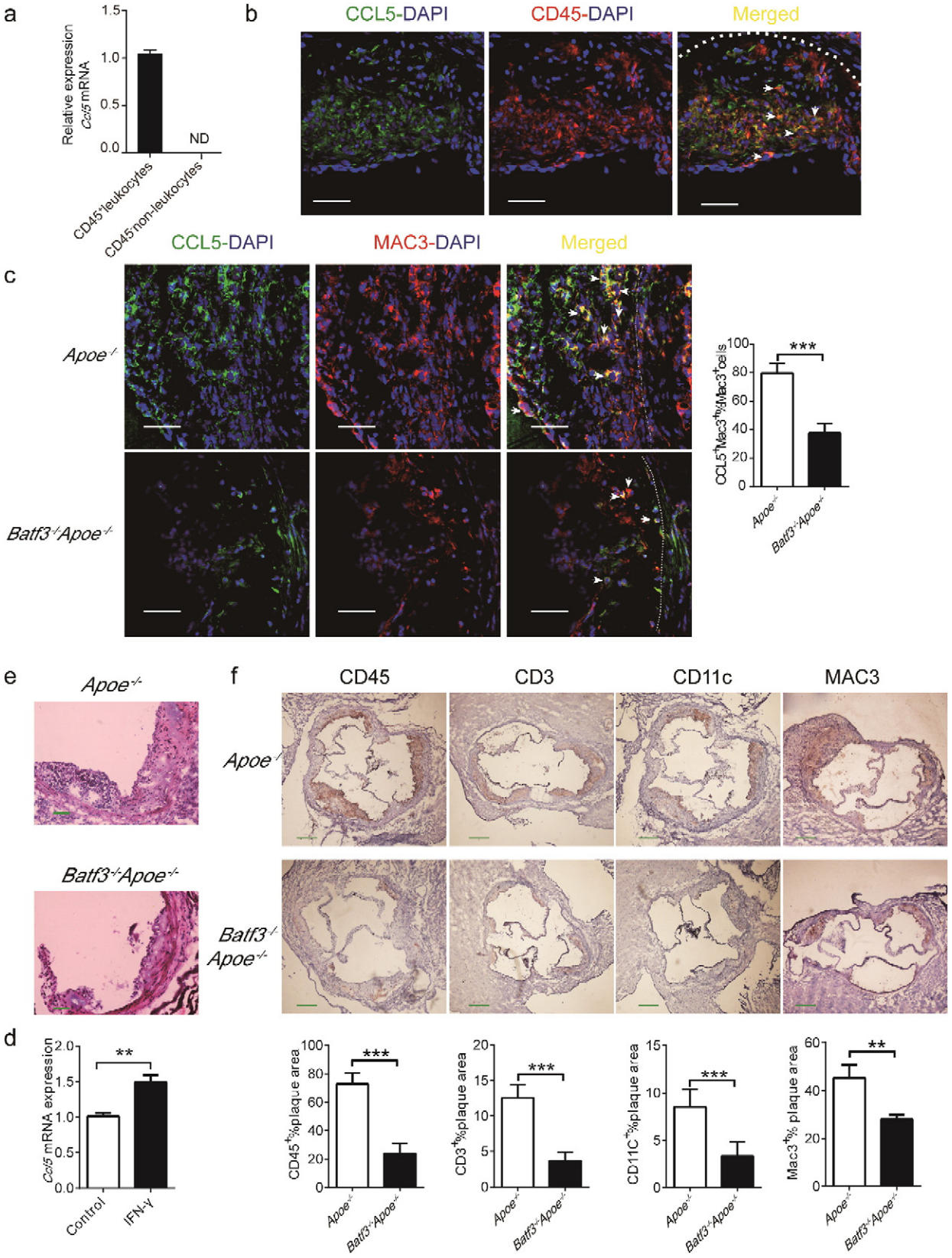

cell response or IFN-γ producing $CD8^+$ T cells response. Conflict with the previous report may be associated with the different methods used to knock out *Batf3* in $Apoe^{-/-}$ mice. During preparation of chimeras, lethal irradiation maybe leads to unknown instability for mice.

It has long been suggested that a Th1 cell response plays a critical role in promoting atherosclerosis (Benagiano et al., 2003; Buono et al., 2005; Laurat et al., 2001; Thacker et al., 2012; Whitman et al., 2000). However, during atherogenesis, how the Th1 cell response is generated, and which DC subset is required for its generation remains unclear. To address this question, we generated $Batf3^{-/-}Apoe^{-/-}$ double knockout mice, and found a significant decrease in Th1 cells but not Th17 cells or Treg cells in the spleen (Fig. 2) in mice selectively depleted of $CD8\alpha^+$ DCs. As a *Batf3* intrinsic deficiency in T cells shown to cause no apparent defect in the development of any known helper T cell subset (Hildner et al., 2008; Murphy et al., 2013), our results demonstrate that $CD8\alpha^+$ DCs are required for the induction of a Th1 cell response under WD conditions. Furthermore, by using a co-culture system, we revealed that splenic $CD8\alpha^+$ DCs from WD fed mice induced an increased Th1 cell response (Fig. 3b, c). These data were consistent with reports that $CD8\alpha^+$ DCs excel in eliciting a Th1 cell response in various settings (Pulendran et al., 1999). Next, we elucidated the mechanism by which $CD8\alpha^+$ DCs induce a Th1 cell response. We found that splenic $CD8\alpha^+$ DCs from WD-exposed mice produced enhanced levels of IL-12, a key Th1 cell polarization cytokine, as analyzed by both qPCR (Fig. 4a) and ELISA (Fig. 4c). As expected, the expression of IL-12p35 was significantly decreased in the aorta of $Batf3^{-/-}Apoe^{-/-}$ mice (Fig. 5c). These data indicate that IL-12 produced by $CD8\alpha^+$ DCs is critical for Th1 cell induction under WD conditions, which were consistent with the reports which suggested Batf3-dependent DCs represent an obligate source of IL-12 to mount protective type I-immunity against the parasitic infections Toxoplasma gondii (Mashayekhi et al., 2011) and Leishmania major (Ashok et al., 2014), but suppress helminth-driven type II immunity (Everts et al., 2016). The mechanism by which a Th1 cell response promotes atherosclerosis remains largely unclear. IFN-γ signaling has many downstream target genes which are potentially relevant to atherosclerosis, particularly those encoding various chemokines (Millward et al., 2007; Wuttge et al., 2004). Thus, we proposed that decreased IFN-γ production caused by $CD8\alpha^+$ DCs ablation could affect the expression of IFN-γ-dependent chemokines in atherosclerosis. As expected, we found the expression of CCL5 (a well known proatherogenic chemokine which promotes plaque formation via recruiting leukocytes to the atherosclerotic aorta) (Braunersreuther et al., 2008; Veillard et al., 2004) was significantly decreased, while no alterations in most of the other chemokines were observed (Fig. S6a), This result suggests that CCL5 expression in the aorta was controlled by Batf3-dependent DCs, which preferentially induced a Th1 cell response.

Although it has been suggested that aortic macrophages were the major CCL5-producing cells in atherosclerotic plaques (Veillard et al., 2004) and was confirmed by our results, it remains unknown how CCL5 expression in macrophages is regulated in atherosclerosis. Interestingly, we found that these CCL5-producing macrophages were significantly reduced in the plaque area of $Batf3^{-/-}Apoe^{-/-}$ mice (Fig. 6c). This finding indicates that $CD8\alpha^+$ DCs play a key role in controlling the expression of CCL5 in atherosclerotic plaque macrophages. We also sought to determine whether IFN-γ promotes CCL5 expression in macrophages in an atherosclerosis-related setting. Interestingly, we found that IFN-γ promoted *Ccl5* expression in the splenic macrophages (Fig. 6d), indicating a direct regulation of CCL5 by IFN-γ. Our data about regulation of CCL5 by IFN-γ was in aggreement with previous documents. For example, intrathecal injection of a replication-defective adenovirus encoding murine IFN (AdIFN) to IFN-γ-deficient mice, induced CCL5 expression in the central nervous system (CNS) in experimental autoimmune encephalomyelitis model (Millward et al., 2007). Furthermore, mice treated with anti-IFN-γ antibody intravaginally for four consecutive days showed decreased CCL5 mRNA expression in vaginal tissues in a lethal herpes simplex virus 2 (HSV-2) infection mice model. Moreover, they also indicated that CCL5 expression was detected in mainly macrophages (Iijima and Iwasaki, 2014) which gave a direct evidence about the regulation of CCL5 by IFN-γ.

Taken together, our data demonstrate an important role of Batf3-dependent $CD8\alpha^+$ DCs in controlling IFN-γ production by Th1 cells and IFN-γ producing $CD8^+$ T cells and IFN-γ-dependent CCL5 expression by plaque macrophages in atherosclerosis. The decrease of $CD8\alpha^+$ DCs-dependent Th1 cells and CCL5 expression likely explains the reduced aortic accumulation of inflammatory leukocytes, and alleviated atherosclerosis. Our data shed light on the important role of Batf3-dependent $CD8\alpha^+$ DCs in promoting the pathogenesis of atherosclerosis.

Funding Sources

This work was supported by grants from the National Basic Research Program of China (2015CB943203), National Natural Science Foundation of China (81302604, 81272315, 81273212), Key Project of Shandong Province for Research and Development (2015GSF118059), Natural Science Foundation of Shandong Province (ZR2011CM037), Science and Technology Development Program of Taian city (2016NS1086, 2015NS2168), and The National High-tech R&D Program (2014ZX09508003).

Conflict of Interest Statement

The authors declare that they have no conflicts of interest.

Author Contributions

Y.L.L. and H.T. designed the experiments. Y.L.L., X.Y.L., W.D., H.T., G.M.Z., H.H., S.Y.Y. and S.T.Y performed the experiments, analyzed and interpreted data. W.G.S. assisted with the experiments and revised the manuscript. Y.L.L and H.T. wrote the manuscript.

Acknowledgements

We thank Na Yuan, Yalu Li and Wenping Sun at the School of Basic Medical Sciences, Taishan Medical University for their technical assistance. We also thank postgraduate student Bin Zhao at Institute of Immunology, Taishan Medical University for his technical assistance.

Fig. 6. IFN-γ promoted CCL5 expression on macrophages, promoting leukocytes infiltration into the plaque area. (a) Female $Apoe^{-/-}$ mice (n = 15) were put on a Western diet for eight weeks, then the aortic cells were pooled to prepared as described in the methods and stained with an antibody against CD45. Then, $CD45^+$ leukocytes and $CD45^-$ non-leukocytes were sorted by FACS, and qPCR was used to analyze *Ccl5* mRNA expression. (b and c) Immunofluorescence of the aortic root. The $Apoe^{-/-}$ mice (n = 8) and the $Batf3^{-/-}Apoe^{-/-}$mice (n = 8) were fed a Western diet for 12 weeks. The cryosections of the aortic root were stained with an antibody against CD45 (red), MAC3 (red), and CCL5 (green). The cell nuclei were counterstained with 4′,6-diamidino-2-phenylindole (DAPI) (blue). Images were viewed and captured with a Laser Scanning Confocal Microscope. Scale bars: 100 μm, dashed lines indicate the internal elastic lamina, arrows pointing to representative colocalized cells. (d) Primary splenic macrophages were sorted as described in supplementary data, and then treated with100 ng/mL IFN-γ for 6 h. *Ccl5* mRNA expression was analyzed by qPCR. The $Apoe^{-/-}$ mice (n = 8) and the $Batf3^{-/-}Apoe^{-/-}$ mice (n = 8) were fed a Western diet for 6 weeks, and cryosections of the aortic root were performed. (e) H&E staining. Scale bars: 100 μm. (f) Immunohistochemistry. Representative images of leukocytes (CD45), T cells (CD3), DCs (CD11c), and macrophages (Mac3) in the aortic are shown. Scale bars: 200 μm. Data are presented as mean ± SD. Differences of a $P < 0.05$ were considered to be statistically significant. $^{**}P < 0.01$; $^{***}P < 0.001$; ns, not significant. Data are representative of three independent experiments.

Appendix A. Supplementary data

Supplementary data to this article can be found online at http://dx.doi.org/10.1016/j.ebiom.2017.04.008.

References

Ashok, D., Schuster, S., Ronet, C., Rosa, M., Mack, V., Lavanchy, C., Marraco, S.F., Fasel, N., Murphy, K.M., Tacchini-Cottier, F., et al., 2014. Cross-presenting dendritic cells are required for control of Leishmania major infection. Eur. J. Immunol. 44, 1422–1432.

Benagiano, M., Azzurri, A., Ciervo, A., Amedei, A., Tamburini, C., Ferrari, M., Telford, J.L., Baldari, C.T., Romagnani, S., Cassone, A., et al., 2003. T helper type 1 lymphocytes drive inflammation in human atherosclerotic lesions. Proc. Natl. Acad. Sci. U. S. A. 100, 6658–6663.

Braunersreuther, V., Steffens, S., Arnaud, C., Pelli, G., Burger, F., Proudfoot, A., Mach, F., 2008. A novel RANTES antagonist prevents progression of established atherosclerotic lesions in mice. Arterioscler. Thromb. Vasc. Biol. 28, 1090–1096.

Buono, C., Binder, C.J., Stavrakis, G., Witztum, J.L., Glimcher, L.H., Lichtman, A.H., 2005. T-bet deficiency reduces atherosclerosis and alters plaque antigen-specific immune responses. Proc. Natl. Acad. Sci. U. S. A. 102, 1596–1601.

Busche, A., Jirmo, A.C., Welten, S.P., Zischke, J., Noack, J., Constabel, H., Gatzke, A.K., Keyser, K.A., Arens, R., Behrens, G.M., et al., 2013. Priming of CD8+ T cells against cytomegalovirus-encoded antigens is dominated by cross-presentation. J. Immunol. 190, 2767–2777.

Chaudhari, S.M., Sluimer, J.C., Koch, M., Theelen, T.L., Manthey, H.D., Busch, M., Caballero-Franco, C., Vogel, F., Cochain, C., Pelisek, J., et al., 2015. Deficiency of HIF1alpha in antigen-presenting cells aggravates atherosclerosis and type 1 T-helper cell responses in mice. Arterioscler. Thromb. Vasc. Biol. 35, 2316–2325.

Chen, K., Zhou, Y.X., Li, K., Qi, L.X., Zhang, Q.F., Wang, M.C., Xiao, J.H., 2016. A novel three-round multiplex PCR for SNP genotyping with next generation sequencing. Anal. Bioanal. Chem. 408, 4371–4377.

Choi, J.H., Cheong, C., Dandamudi, D.B., Park, C.G., Rodriguez, A., Mehandru, S., Velinzon, K., Jung, I.H., Yoo, J.Y., Oh, G.T., et al., 2011. Flt3 signaling-dependent dendritic cells protect against atherosclerosis. Immunity 35, 819–831.

Cipriani, S., Francisci, D., Mencarelli, A., Renga, B., Schiaroli, E., D'Amore, C., Baldelli, F., Fiorucci, S., 2013. Efficacy of the CCR5 antagonist maraviroc in reducing early, ritonavir-induced atherogenesis and advanced plaque progression in mice. Circulation 127, 2114–2124.

Combadiere, C., Potteaux, S., Rodero, M., Simon, T., Pezard, A., Esposito, B., Merval, R., Proudfoot, A., Tedgui, A., Mallat, Z., 2008. Combined inhibition of CCL2, CX3CR1, and CCR5 abrogates Ly6C(hi) and Ly6C(lo) monocytosis and almost abolishes atherosclerosis in hypercholesterolemic mice. Circulation 117, 1649–1657.

Edelson, B.T., Kc, W., Juang, R., Kohyama, M., Benoit, L.A., Klekotka, P.A., Moon, C., Albring, J.C., Ise, W., Michael, D.G., et al., 2010. Peripheral CD103+ dendritic cells form a unified subset developmentally related to CD8alpha+ conventional dendritic cells. J. Exp. Med. 207, 823–836.

Everts, B., Tussiwand, R., Dreesen, L., Fairfax, K.C., Huang, S.C., Smith, A.M., O'Neill, C.M., Lam, W.Y., Edelson, B.T., Urban Jr., J.F., et al., 2016. Migratory CD103+ dendritic cells suppress helminth-driven type 2 immunity through constitutive expression of IL-12. J. Exp. Med. 213, 35–51.

Gautier, E.L., Huby, T., Saint-Charles, F., Ouzilleau, B., Pirault, J., Deswaerte, V., Ginhoux, F., Miller, E.R., Witztum, J.L., Chapman, M.J., et al., 2009. Conventional dendritic cells at the crossroads between immunity and cholesterol homeostasis in atherosclerosis. Circulation 119, 2367–2375.

Gupta, S., Pablo, A.M., Jiang, X., Wang, N., Tall, A.R., Schindler, C., 1997. IFN-gamma potentiates atherosclerosis in ApoE knock-out mice. J. Clin. Invest. 99, 2752–2761.

He, H., Geng, T., Chen, P., Wang, M., Hu, J., Kang, L., Song, W., Tang, H., 2016. NK cells promote neutrophil recruitment in the brain during sepsis-induced neuroinflammation. Sci. Rep. 6, 27711.

Heller, E.A., Liu, E., Tager, A.M., Yuan, Q., Lin, A.Y., Ahluwalia, N., Jones, K., Koehn, S.L., Lok, V.M., Aikawa, E., et al., 2006. Chemokine CXCL10 promotes atherogenesis by modulating the local balance of effector and regulatory T cells. Circulation 113, 2301–2312.

Hildner, K., Edelson, B.T., Purtha, W.E., Diamond, M., Matsushita, H., Kohyama, M., Calderon, B., Schraml, B.U., Unanue, E.R., Diamond, M.S., et al., 2008. Batf3 deficiency reveals a critical role for CD8alpha+ dendritic cells in cytotoxic T cell immunity. Science 322, 1097–1100.

Huang, L.Y., Reis e Sousa, C., Itoh, Y., Inman, J., Scott, D.E., 2001. IL-12 induction by a TH1-inducing adjuvant in vivo: dendritic cell subsets and regulation by IL-10. J. Immunol. 167, 1423–1430.

Iijima, N., Iwasaki, A., 2014. T cell memory. A local macrophage chemokine network sustains protective tissue-resident memory CD4 T cells. Science 346, 93–98.

Iqbal, J., Queiroz, J., Li, Y., Jiang, X.C., Ron, D., Hussain, M.M., 2012. Increased intestinal lipid absorption caused by Ire1beta deficiency contributes to hyperlipidemia and atherosclerosis in apolipoprotein E-deficient mice. Circ. Res. 110, 1575–1584.

Kawka, E., Witowski, J., Fouqet, N., Tayama, H., Bender, T.O., Catar, R., Dragun, D., Jorres, A., 2014. Regulation of chemokine CCL5 synthesis in human peritoneal fibroblasts: a key role of IFN-gamma. Mediat. Inflamm. 2014, 590654.

Koltsova, E.K., Garcia, Z., Chodaczek, G., Landau, M., McArdle, S., Scott, S.R., von Vietinghoff, S., Galkina, E., Miller, Y.I., Acton, S.T., et al., 2012. Dynamic T cell-APC interactions sustain chronic inflammation in atherosclerosis. J. Clin. Invest. 122, 3114–3126.

Lahoute, C., Herbin, O., Mallat, Z., Tedgui, A., 2011. Adaptive immunity in atherosclerosis: mechanisms and future therapeutic targets. Nat. Rev. Cardiol. 8, 348–358.

Laurat, E., Poirier, B., Tupin, E., Caligiuri, G., Hansson, G.K., Bariety, J., Nicoletti, A., 2001. In vivo downregulation of T helper cell 1 immune responses reduces atherogenesis in apolipoprotein E-knockout mice. Circulation 104, 197–202.

Legein, B., Janssen, E.M., Theelen, T.L., Gijbels, M.J., Walraven, J., Klarquist, J.S., Hennies, C.M., Wouters, K., Seijkens, T.T., Wijnands, E., et al., 2015. Ablation of CD8alpha(+) dendritic cell mediated cross-presentation does not impact atherosclerosis in hyperlipidemic mice. Sci. Rep. 5, 15414.

Leventhal, D.S., Gilmore, D.C., Berger, J.M., Nishi, S., Lee, V., Malchow, S., Kline, D.E., Kline, J., Vander Griend, D.J., Huang, H., et al., 2016. Dendritic cells coordinate the development and homeostasis of organ-specific regulatory T cells. Immunity 44, 847–859.

Liu, K., Nussenzweig, M.C., 2010. Origin and development of dendritic cells. Immunol. Rev. 234, 45–54.

Liu, J., Guan, X., Ma, X., 2005. Interferon regulatory factor 1 is an essential and direct transcriptional activator for interferon {gamma}-induced RANTES/CCl5 expression in macrophages. J. Biol. Chem. 280, 24347–24355.

Mashayekhi, M., Sandau, M.M., Dunay, I.R., Frickel, E.M., Khan, A., Goldszmid, R.S., Sher, A., Ploegh, H.L., Murphy, T.L., Sibley, L.D., et al., 2011. CD8alpha(+) dendritic cells are the critical source of interleukin-12 that controls acute infection by toxoplasma gondii tachyzoites. Immunity 35, 249–259.

Mildner, A., Jung, S., 2014. Development and function of dendritic cell subsets. Immunity 40, 642–656.

Millward, J.M., Caruso, M., Campbell, I.L., Gauldie, J., Owens, T., 2007. IFN-gamma-induced chemokines synergize with pertussis toxin to promote T cell entry to the central nervous system. J. Immunol. 178, 8175–8182.

Moore, K.J., Tabas, I., 2011. Macrophages in the pathogenesis of atherosclerosis. Cell 145, 341–355.

Murphy, T.L., Tussiwand, R., Murphy, K.M., 2013. Specificity through cooperation: BATF-IRF interactions control immune-regulatory networks. Nat. Rev. Immunol. 13, 499–509.

Pulendran, B., Smith, J.L., Caspary, G., Brasel, K., Pettit, D., Maraskovsky, E., Maliszewski, C.R., 1999. Distinct dendritic cell subsets differentially regulate the class of immune response in vivo. Proc. Natl. Acad. Sci. U. S. A. 96, 1036–1041.

Rolin, J., Maghazachi, A.A., 2014. Implications of chemokines, chemokine receptors, and inflammatory lipids in atherosclerosis. J. Leukoc. Biol. 95, 575–585.

Sage, A.P., Murphy, D., Maffia, P., Masters, L.M., Sabir, S.R., Baker, L.L., Cambrook, H., Finigan, A.J., Ait-Oufella, H., Grassia, G., et al., 2014. MHC class II-restricted antigen presentation by plasmacytoid dendritic cells drives proatherogenic T cell immunity. Circulation 130, 1363–1373.

Schmittgen, T.D., Livak, K.J., 2008. Analyzing real-time PCR data by the comparative C(T) method. Nat. Protoc. 3, 1101–1108.

Schroder, K., Hertzog, P.J., Ravasi, T., Hume, D.A., 2004. Interferon-gamma: an overview of signals, mechanisms and functions. J. Leukoc. Biol. 75, 163–189.

Shamshiev, A.T., Ampenberger, F., Ernst, B., Rohrer, L., Marsland, B.J., Kopf, M., 2007. Dyslipidemia inhibits toll-like receptor-induced activation of CD8alpha-negative dendritic cells and protective Th1 type immunity. J. Exp. Med. 204, 441–452.

Smith, E., Prasad, K.M., Butcher, M., Dobrian, A., Kolls, J.K., Ley, K., Galkina, E., 2010. Blockade of interleukin-17A results in reduced atherosclerosis in apolipoprotein E-deficient mice. Circulation 121, 1746–1755.

Soares, H., Waechter, H., Glaichenhaus, N., Mougneau, E., Yagita, H., Mizenina, O., Dudziak, D., Nussenzweig, M.C., Steinman, R.M., 2007. A subset of dendritic cells induces CD4+ T cells to produce IFN-gamma by an IL-12-independent but CD70-dependent mechanism in vivo. J. Exp. Med. 204, 1095–1106.

Stewart, C.R., Stuart, L.M., Wilkinson, K., van Gils, J.M., Deng, J., Halle, A., Rayner, K.J., Boyer, L., Zhong, R., Frazier, W.A., et al., 2010. CD36 ligands promote sterile inflammation through assembly of a toll-like receptor 4 and 6 heterodimer. Nat. Immunol. 11, 155–161.

Subramanian, M., Thorp, E., Hansson, G.K., Tabas, I., 2013. Treg-mediated suppression of atherosclerosis requires MYD88 signaling in DCs. J. Clin. Invest. 123, 179–188.

Suffee, N., Hlawaty, H., Meddahi-Pelle, A., Maillard, L., Louedec, L., Haddad, O., Martin, L., Laguillier, C., Richard, B., Oudar, O., et al., 2012. RANTES/CCL5-induced pro-angiogenic effects depend on CCR1, CCR5 and glycosaminoglycans. Angiogenesis 15, 727–744.

Tabas, I., Bornfeldt, K.E., 2016. Macrophage phenotype and function in different stages of atherosclerosis. Circ. Res. 118, 653–667.

Thacker, S.G., Zhao, W., Smith, C.K., Luo, W., Wang, H., Vivekanandan-Giri, A., Rabquer, B.J., Koch, A.E., Pennathur, S., Davidson, A., et al., 2012. Type I interferons modulate vascular function, repair, thrombosis, and plaque progression in murine models of lupus and atherosclerosis. Arthritis Rheum. 64, 2975–2985.

Veillard, N.R., Kwak, B., Pelli, G., Mulhaupt, F., James, R.W., Proudfoot, A.E., Mach, F., 2004. Antagonism of RANTES receptors reduces atherosclerotic plaque formation in mice. Circ. Res. 94, 253–261.

Vignali, D.A., Kuchroo, V.K., 2012. IL-12 family cytokines: immunological playmakers. Nat. Immunol. 13, 722–728.

Wang, Y., Wang, G.Z., Rabinovitch, P.S., Tabas, I., 2014. Macrophage mitochondrial oxidative stress promotes atherosclerosis and nuclear factor-kappaB-mediated inflammation in macrophages. Circ. Res. 114, 421–433.

Weber, C., Meiler, S., Doring, Y., Koch, M., Drechsler, M., Megens, R.T., Rowinska, Z., Bidzhekov, K., Fecher, C., Ribechini, E., et al., 2011. CCL17-expressing dendritic cells drive atherosclerosis by restraining regulatory T cell homeostasis in mice. J. Clin. Invest. 121, 2898–2910.

Whitman, S.C., Ravisankar, P., Elam, H., Daugherty, A., 2000. Exogenous interferon-gamma enhances atherosclerosis in apolipoprotein E−/− mice. Am. J. Pathol. 157, 1819–1824.

Wuttge, D.M., Zhou, X., Sheikine, Y., Wagsater, D., Stemme, V., Hedin, U., Stemme, S., Hansson, G.K., Sirsjo, A., 2004. CXCL16/SR-PSOX is an interferon-gamma-regulated chemokine and scavenger receptor expressed in atherosclerotic lesions. Arterioscler. Thromb. Vasc. Biol. 24, 750–755.

Xu, Y., Liu, Y., Yang, C., Kang, L., Wang, M., Hu, J., He, H., Song, W., Tang, H., 2016. Macrophages transfer antigens to dendritic cells by releasing exosomes containing dead-cell-associated antigens partially through a ceramide-dependent pathway to enhance CD4(+) T-cell responses. Immunology 149, 157–171.